The Effect of Cooling Wall Locations on Electronics Cooling Using Nanofluids

Dr. Said A. El. Agous *Dr. Husni T. Izweik*
Department of mechanical Engineering *Department of mechanical Engineering*
Zawia University

ABSTRACT:

This work presents a numerical study of natural convection cooling of a heated block embedded in the bottom wall of an enclosure filled with nanofluids. A constant and uniform heat generation rate is produced inside the block. The influence of Rayleigh number, the local cooling walls of the enclosure, the type of nanofluid and solid volume fraction of nanoparticles on the cooling performance is studied. Four cases of local cooling walls are carried out to find the best location. The results indicate that qualitatively similar trends in isotherms and streamlines are observed for nanofluids and water. Case 2 has the highest cooling performance for different value of

Rayleigh number and volume fraction while, case 3 has the lowest cooling performance for Cu nanoparticle. The enhancement in the maximum temperature for case 2 when the volume fraction of nanoparticles is increased from 0 to 0.2, at Ra = 10^3, is approximately 39.4%, whereas the enhancement is around 26.2% at Ra = 10^6 for Cu nanoparticle. In ϕ= 0.2 and case 2, the maximum temperature and average Nusselt number are constant for Ra $\leq 10^5$ after this value the maximum temperature decreases and average Nusselt number increases for considering nanoparticles.

Keywords: Natural convection; enclosure; heat generation; nanofluids; heat transfer

Nomenclature:

A	Aspect ratio of the enclosure (W/H)
C_p	Specific heat at constant pressure (kJ kg^{-1} K^{-1})
g	Modulus of the gravity vector (g =9.81 m/s^2)
Gr	Grashof number
h	Local heat transfer coefficient (Wm^{-2} K^{-1})
H	Height of the enclosure (m)
h	Height of the heated block (m)
k	Thermal conductivity (W m^{-1} K^{-1})
Nu	Nusselt number, Nu = hH/k
Pr	Prandtl number
q'''	Uniform heat generation rate (W m^{-3})
Ra	Rayleigh number
T	dimensional temperature (K)
U, V	Dimensionless velocities in *X, Y* directions

u, v	Velocity components in *x, y* directions (m s^{-1})
W	Width of the enclosure (m)
w	Width of the heated block (m)
x, y	Cartesian coordinates (m)
X, Y	Dimensionless Cartesian coordinates

Greek symbols:

ψ	Dimensionless stream function
θ	Dimensionless temperature
ω	Dimensionless vorticity
Φ	General variable
ν	Kinematic viscosity (m^2 s^{-1})
ϕ	Nanoparticle volume fraction
α	Thermal diffusivity (m^2 s^{-1})
ρ	Density (kg m^{-3})
β	thermal expansion coefficient (K^{-1})

Subscripts:

avg	Average
c	Ambient
f	Fluid
h	Heated block
nf	Nanofluid
s	Solid
w	Wall

1. Introduction:

Nanofluid becomes more attractive in recent years due to easy production methods and the inexpensive price. Also, thermal conductivity of nanofluids relative to the base fluids is very high. Thus, nanofluids can be applied in many exegetical systems such as cooling of nuclear systems, radiators, natural convection in enclosures. The natural convection heat transfer is an important observable fact, in engineering systems due to its extensive applications in heat exchangers, double pane windows, and insulations. Many researchers considered Nanotechnology as the most important driving moment for the major industrial revolution of this century. The low thermal conductivity of conventional fluids such as water, oil, air, and ethylene glycol mixture is considered as the primary obstacle to enhance the performance of heat exchangers.

Some review papers that show applications and detail solutions on nanofluids Daungthongsuk ; Wongwises, (2007), Trisaksri ; Wongwises, (2007) and Kleinstreuer ; Feng, (2011). Natural convection in horizontal annuli used different types of water based-nanofluids studied by Abu-Nada, et al. (2010) and they observed that addition of nanoparticles into base fluid enhances the heat transfer.

Several studies were performed on natural convection using Nano-fluids in cavities. Khanafer, et al. (2003) investigated the heat transfer enhancement in a two-dimensional enclosure utilizing Nano-fluids for various pertinent parameters. These authors reported an augmentation in heat transfer with an incremental percentage of the suspended nanoparticles at any given Grashof number. Hwang, et al. (2007) investigated the buoyancy-driven heat transfer of water-based Al_2O_3 Nano-fluids in a rectangular cavity. Jou, and Tzeng, (2006) used Nano-fluids to enhance natural convection heat transfer in a rectangular enclosure. They indicated

that the volume fraction of Nano-fluids causes an increase in the average heat transfer coefficient. Oztop and Abu-Nada, (2008); investigated heat transfer and fluid flow due to buoyancy forces in a partially heated enclosure using different nanofluids. The flush mounted heater was located in the left vertical wall with a finite length. The temperature of vertical wall was lower than that of heater while other walls were insulated. Calculations were performed for different height of heater, location of heater, Rayleigh numbers, aspect ratio and volume fraction of nanoparticles. They found that heat transfer increases with increasing height of the heater, Rayleigh number and volume fraction of nanoparticles. In addition, the heat transfer enhancement was found to be dependent on the type of nanofluid and more pronounced at low aspect ratio that at high aspect ratio. The numerical studies on nanofluid increases in recent years for different models and different configurations. Ögüt, (2009) studied numerically the natural convection heat transfer of water-based nanofluids in an inclined enclosure with a constant flux heater. Five types of nanoparticles were taken into consideration: Cu, CuO, Al_2O_3 and TiO_2. The results showed that the average heat transfer rate increases significantly as Rayleigh number and particle volume fraction increase, the effect is more pronounced for Ag and Cu nanoparticles. The results also showed that the average heat transfer decreases with an increase in the length of the heater. Abu-Nada, et al. (2008) demonstrated that the enhancement of heat transfer in natural convection depends mainly on the magnitude of Rayleigh number. In fact, for a certain Rayleigh number, like $Ra \leq 10^4$, the heat transfer was not sensitive to nanoparticles, whereas at higher values of Rayleigh number, an enhancement in heat transfer was observed. Therefore, there is still a controversy on the role of nanofluid in natural convection heat transfer where the numerical simulations seem to overestimate the level of

enhancement. Natural convection in a partially heated enclosure from below and filled with different types of nanofluids was numerically studied by Aminossadati and Ghasemi, (2009). The effects of solid volume fraction, Rayleigh number, heat source length and location and the type of nanofluid on the enclosure cooling performance were presented. The results indicated that the addition of 20% of Cu and Ag nanoparticles in pure water the increased cooling performance by 42.8%. The length and location of the heat source proved to significantly affect the heat source maximum temperature. Ghasemi and Aminossadati, (2010) studied natural convection cooling of an oscillating heat source embedded on the left wall of an enclosure filled with nanofluids numerically. The effects of various pertinent parameters such as heat source position, Rayleigh number, solid volume fraction, type of nanofluid and the oscillation period on the cooling performance of the enclosure are examined. The study showed that at low Rayleigh numbers, where the conduction is the main heat transfer mechanism, this effect is more noticeable such that the addition of 20% Cu nanoparticles results in a 37% reduction of the heat source maximum temperature. The influence of the heat source position is a function of Rayleigh number. Sheikhzadeh, et al. (2011) numerically modeled the buoyancy-driven fluid flow and heat transfer in a square cavity with partially active side walls filled with Cu–water nanofluid. They studied the effects of the position of the active portions of the side walls, and volume fraction. The result showed that the average Nusselt number increases with increasing both the Rayleigh number and the volume fraction. Moreover, the maximum average Nusselt number for the high and the low Rayleigh numbers occur in the bottom-middle and the middle–middle locations of the thermally active parts, respectively. Ghasemi, and Aminossadati, (2010) presented study of a numerical study on the natural convection in a

right triangular enclosure, with a heat source on its vertical wall and filled with a water–Cuo nanofluid. It was noticed that when Brownian motion is neglected, the heat transfer rate continuously increases with increasing the solid volume fraction at all Rayleigh numbers. A natural convection of CuO–water nanofluid in a cavity with two pairs of heat source–sink which cover the bottom wall and the remaining walls are insulated has been investigated by Aminossadati, and Ghasemi, (2011). A comparison study is presented between two cases corresponding at different arrangements of the two active sources. It was found that increasing the nanoparticle volume fraction and Rayleigh number leads to a strong increase of the heat transfer rate. The natural convection in an enclosure with a heat source located at its bottom wall and filled with an Ethylene Glycol–Cu nanofluid studied numerically by Aminossadati, and Ghasemi, (2011). The results indicated that with an increase in the Rayleigh number and solid volume fraction the thermal performance of the enclosure is improved. The variation of heat transfer rate with respect to the enclosure apex angle, heat source position and dimensions is different at low and high Rayleigh numbers.

Previous works investigations have merely focused on momentum and energy transfer in enclosure subjected to prescribed temperature and prescribed wall heat flux. However, only a very limited amount of numerical work on momentum and energy transfer in enclosure subjected heat generation and cooling wall locations on natural convection of water-based nanofluids. The main aim of this work is to study natural convection heat transfer around the heated block in enclosures filled with nanofluid numbing. A constant and uniform heat generation rate is produced inside the block. The effects of the Rayleigh number, the volume fraction of the nanoparticle and the local cooling walls of the enclosure on maximum temperature and Nusselt number are investigated. The effects of water-Cu

nanofluids on flow and temperature fields is presented. Four cases of local cooling walls are carried out to find the best location. After obtaining best case, the comparison between three different nanofluids such as Cu, Al_2O_3, and TiO_3 are tested. The mentioned literature survey indicates that there is no study on natural convection in an enclosure filled with heated block and nanofluid.

2. Mathematical modeling:

Fig. 1 shows the schematic diagram of the physical configuration and considered cases of the enclosure having width W and height H. A constant and uniform heat generation rate (q''') is produced inside the block width w_h, height h_h, and thermal conductivity k_h. In case 1, the lower and upper wall surfaces are assumed to be adiabatic where the side walls of the enclosure are maintained at ambient temperature T_c. In case 2, the lower and upper wall surfaces are maintained at ambient temperature T_c except, the heat source is assumed to be adiabatic where the side walls of the enclosure are assumed to be adiabatic. In case 3, the upper wall surface is maintained at ambient temperature T_c where the lower and side walls of the enclosure are assumed to be adiabatic. In case 4, the lower wall surface is maintained at ambient temperature T_c except, the heat source is assumed to be adiabatic where the upper and side walls of the enclosure are assumed to be adiabatic. The fluid in the enclosure is a water-based nanofluid containing Cu or Al_2O_3 or TiO_3 nanoparticles and they are assumed incompressible. It is idealized that water and nanoparticles are in thermal equilibrium and no slip occurs between the two media. The thermo-physical properties of the nanofluid are listed in Table 1 Khanafer, et al. (2003) and Abu-Nada, et al. (2010). The density of the nanofluid is

approximated by the standard Boussinesq model. The viscosity and the thermal conductivity of the nanofluid are considered as variable properties; both vary with the volume fraction of nanoparticles. The continuity, momentum under Boussinesq approximation and energy equations for the laminar and steady-state natural convection in the two-dimensional enclosure can be written in dimensional form as follows:

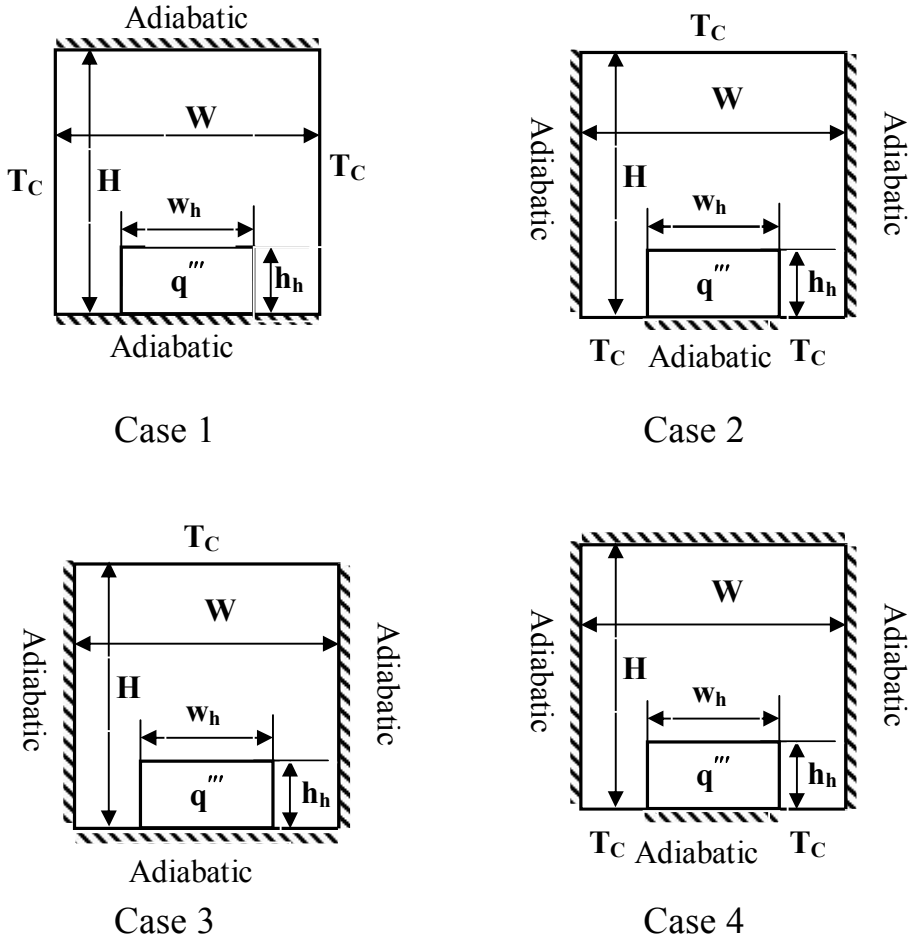

Fig. 1 Schematic for the physical configuration and considered cases.

Table 1 Thermophysical properties of pure water and nanoparticle

Physical properties	Pure water	Cu	Al_2O_3	TiO_3
C_p (j/kg k)	4197	385	765	686.2
ρ (kg/m^3)	997.1	8933	3970	4250
K (W/m k)	0.613	400	40	8.9538
β ×10^{-5} (k^{-1})	21	1.67	0.85	0.9
α×10^7 (m^2/s)	1.47	1163.1	131.7	30.7

Continuity equation

$$\frac{\partial u}{\partial x}+\frac{\partial v}{\partial y}=0 \qquad (1)$$

Momentum equations

$$u\frac{\partial u}{\partial x}+v\frac{\partial u}{\partial y}=-\frac{1}{\rho_{nf}}\left(\frac{\partial p}{\partial x}\right)+\frac{\mu_{nf}}{\rho_{nf}}\left[\frac{\partial^2 u}{\partial x^2}+\frac{\partial^2 u}{\partial y^2}\right] \qquad (2)$$

$$u\frac{\partial v}{\partial x}+v\frac{\partial v}{\partial y}=-\frac{1}{\rho_{nf}}\left(\frac{\partial p}{\partial x}\right)+\frac{\mu_{nf}}{\rho_{nf}}\left[\frac{\partial^2 v}{\partial x^2}+\frac{\partial^2 v}{\partial y^2}\right]+g\beta_{nf}(T-T_C) \qquad (3)$$

Energy equations

For nanofluid flow $$u\frac{\partial T}{\partial x}+v\frac{\partial T}{\partial y}=\alpha_{nf}\left[\frac{\partial^2 T}{\partial x^2}+\frac{\partial^2 T}{\partial y^2}\right] \qquad (4)$$

For heated block $$\left[\frac{\partial^2 T}{\partial x^2}+\frac{\partial^2 T}{\partial y^2}\right]+\frac{q'''}{k_h}=0 \qquad (5)$$

Where the effective density (ρ_{nf}), heat capacitance $(\rho C_p)_{nf}$, thermal expansion coefficient *(β_{nf}), and* thermal diffusivity *(α_{nf})* of the nanofluid are defined as [15]:

$$\rho_{nf}=(1-\phi)\,\rho_f+\phi\rho_s \qquad (6)$$

$$(\rho C_p)_{nf} = (1-\phi)\,(\rho C_p)_f + \phi\,(\rho C_p)_s \quad (7)$$

$$\beta_{nf} = (1-\phi)\,\beta_f + \phi\,\beta_s \quad (8)$$

And

$$\alpha_{nf} = \frac{k_{nf}}{(\rho C_p)_{nf}} \quad (9)$$

Where ϕ is the volume fraction of nanoparticles.

The dynamic viscosity of the nanofluids given by Brinkman [23] is:

$$\mu_{nf} = \frac{\mu_f}{(1-\phi)^{2.5}} \quad (10)$$

The effective thermal conductivity of the nanofluid can be approximated by the Maxwell–Garnetts (MG) model:

$$\frac{k_{nf}}{k_f} = \frac{k_s + 2k_f - 2\phi\,(k_f - k_s)}{k_s + 2k_f + 2\phi\,(k_f - k_s)} \quad (11)$$

The governing equations of continuity, momentum and energy (1-5) can be transformed to the dimensionless form, with the dimensionless variables defined as:

$$X = \frac{x}{H},\ Y = \frac{y}{H},\ H_h = \frac{h_h}{H},\ W_h = \frac{w_h}{H},\ U = \frac{uH}{\alpha_f},\ V = \frac{vH}{\alpha_f},\ \theta = \frac{T - T_c}{q'''\,h_h w_h / k_f}$$

And then, the vorticity equation is obtained by eliminating the pressure between the two momentum equations, i.e. by taking y-derivative of Eq.(2) and subtracting from it the x-derivative of Eq.(3). This gives:

$$U\frac{\partial \omega}{\partial X} + V\frac{\partial \omega}{\partial Y} = \left[\frac{Pr_f}{(1-\phi)^{2.5}\left((1-\phi) + \phi\frac{\rho_s}{\rho_f}\right)}\right]\left[\frac{\partial^2 \omega}{\partial X^2} + \frac{\partial^2 \omega}{\partial Y^2}\right]$$

$$+ Ra_f\,Pr_f\left[\left(\frac{1}{\frac{(1-\phi)}{\phi}\frac{\rho_s}{\rho_f} + 1}\right)\left(\frac{\beta_s}{\beta_f}\right) + \left(\frac{1}{\frac{\phi}{(1-\phi)}\frac{\rho_s}{\rho_f} + 1}\right)\right]\frac{\partial \theta}{\partial X} \quad (12)$$

$$U\frac{\partial\theta}{\partial X}+V\frac{\partial\theta}{\partial Y}=\left[\frac{\frac{K_{nf}}{K_f}}{(1-\phi)+\phi\frac{(\rho C_p)_s}{(\rho C_p)_f}}\right]\left[\frac{\partial^2\theta}{\partial X^2}+\frac{\partial^2\theta}{\partial Y^2}\right] \quad (13)$$

$$\left[\frac{\partial^2\theta}{\partial X^2}+\frac{\partial^2\theta}{\partial Y^2}\right]+\frac{k_f}{k_h}\frac{1}{W_h H_h}=0 \quad (14)$$

$$-\omega=\left[\frac{\partial^2\psi}{\partial X^2}+\frac{\partial^2\psi}{\partial Y^2}\right] \quad (15)$$

The dimensionless stream function and vorticity used in Eqs. (13) and (14) are defined as follows:

$$U=\frac{\partial\psi}{\partial Y},\ V=-\frac{\partial\psi}{\partial X} \quad (16)$$

where $Ra_f=g\beta_f q''' h_h w_h H^3/\alpha_f \upsilon_f$ is the Rayleigh number for the base fluid, and $Pr_f=v_f/\alpha_f$ is the Prandtl number for the base fluid.

Equations (12-16) represent the model governing equations, which are function of the dimensionless the vorticity ω, temperature θ, the stream function ψ, and velocities U and V

The local Nusselt number along the surface of the heat block covered with nanofluids can be expressed as:

$$Nu_x=-\frac{(k_{nf}/k_f)}{\theta_w}\left[\frac{\partial\theta}{\partial n}\right]_w \quad (17)$$

where "n" is the coordinate normal to the wall of heated block

The mean Nusselt number can be calculated as follows:

$$Nu_m=\frac{1}{A}\int_A Nu_x\, dA \quad (18)$$

where A is the surface area exposed to the fluid.

The dimensionless boundary conditions are written as

1- On the adiabatic wall i.e. U = V = ψ =0,∂θ/∂n=0 (19)

2- On the cooling wall i.e. U = V = ψ =0, θ=0 (20)

3- The dimensionless matching interface conditions for any two different media i.e.,

$$-\frac{k_1}{k_f}\frac{\partial\theta}{\partial n}\bigg|_1+\frac{k_2}{k_f}\frac{\partial\theta}{\partial n}\bigg|_2+\frac{\Delta n}{2L_sT_s}\bigg|_2=0,\quad \theta_1=\theta_2 \qquad (21)$$

where k_1 is the thermal conductivity of water or nanofluids and k_2 is the thermal conductivity of heated block.

3. Numerical procedure and grid testing:

The governing equations (12-14) with corresponding boundary conditions given in Eqs. (19-21) are solved using the finite volume approach by Patankar, (1980) and Versteeg, and Malalasekera, (2007) has been used for discretizing the governing equations. The computational domain in two dimensions has been discretised using control volumes of uniform size. Convection–diffusion terms have been treated by the upwind scheme and diffusion and source terms have been treated by the central differencing scheme. The governing equations are integrated over the control volume with the use of linear interpolation inside the finite element, and the obtained algebraic equations are solved by the Gauss–Seidel method. The above mentioned numerical method has been implemented in a self-written FORTRAN computer code which, solve non-linear partial differential equations in two dimensions. The convergence criterion used for all field variables (Φ = ψ, ω, θ) for the termination of all computations is:

$$\varepsilon=\left|(\Phi_{n+1}-\Phi_n)/\Phi_n\right|_{max}\leq 10^{-6}$$

where ε is the tolerance and *n* is the index representing the number of iterations.

In the present paper, uniform mesh distribution is used throughout the domain. Computations are performed with various grid densities 81×81, 97×97, 101×101, and 121×121 for the case of Ra=10^5 and ϕ = 0.1 for Cu–water nanofluid. The present code was tested for grid independence by calculating the average Nusselt number on the walls and a maximum temperature of heat block. Table 2 summarizes the results of the grid-independent test in the present computations. As noted from Table 2,it is observed that difference between the results of the grid 101×101 and that of the grid 97×97 is less than 0.76 and 0.6 % for Nusselt number and maximum temperature. So, it is used (101×101) in the present computation.

Table 2. Grid independency for water-based copper nanofluid at Ra=10^5 and ϕ = 0.1

Grid	Nu_{ave}	Error,%	θ_{max}	Error,%
81×81	12.0822	-	0.1192	-
97×97	12.5092	3.53	0.1153	3.27
101×101	12.6043	0.76	0.1146	0.6
121×121	12.348	2.03	0.1161	1.31

4. Code validation:

The present numerical solution was further validated by comparing the present code results for Ra =10^5 and Pr = 0.70 with the experimental results of Krane and Jessee (1983) and the numerical simulation of Khanafer et al. (2003) and Oztop and Abu-Nada, (2008). It is evident that the outcome of present code is in good agreement with the present work reported in the literature as shown in Fig. 2.

Fig. 3 shows a comparison between present work (plotted by dashed lines) and Oztop, and Abu-Nada (2008) (plotted by solid lines) on

streamlines (on the left) and isotherms (on the right) using different values of nanoparticle volume fraction. As seen in, Fig. 3 the agreement between the results is good agreement. Therefore, the numerical code is reliable and can predict natural convection in enclosures. Also the present code is validated in El-Agouz (2008).

5. Results and discussions:

In the present study, the aspect ratio of the enclosure is A=1. The dimensionless width W_h, height H_h, and thermal conductivity k_h/k_f of heated block are 0.5 , 0.25 and 16.31 respectively. Prandtl number of pure water 6.2. The nanoparticle volume fraction ϕ, is varied from 0.0 to 0.2. Rayleigh number varied from 10^3 to 10^6.

5.1. The effect of Rayleigh number for different cases:

Figs. 4 and 5 displays streamlines and isotherms in the enclosure for the pure water case for various values of Rayleigh numbers and all cases. Since the heat source is located in the middle of the bottom wall, symmetrical flow and temperature patterns are observed in the enclosure. The figure demonstrates that the two counter-rotating rotation cells within the enclosure are intensified for all values of Rayleigh numbers and all cases. By increasing the value of Rayleigh number the buoyant force becomes stronger, velocity increases and the boundary layers become more distinguished for all values of Rayleigh numbers and all cases. It must be noted that the contact line of the symmetrical circulation zones agrees with the axis of symmetry of the heat source for all Rayleigh numbers except at $Ra=10^6$ for case 2 and 3, the cell on the left fills the cavity more than the one on the right. It may be noted that, the maximum ψ= 4.64, 4, 6.55 and

0.56 for cases 1, 2, 3 and 4, respectively at Ra = 10^5 whereas the corresponding values of ψ are 14.53, 19.22, 25.89 and 2.06 at Ra = 10^6.

As shown in Fig. 5, the isotherms also have symmetrical shape at each Ra, however, they display different behaviors as Rayleigh number changes. For the cases of Ra =10^3 and 10^4, where conduction dominates the flow regime, the isotherms are distributed near the heat source. As the Rayleigh number increases, streamlines exhibit stronger flow patterns and isotherms display more distinguished boundary layers. It must be noted that the contact line of the symmetrical zones agrees with the axis of symmetry of the heat source for all Rayleigh numbers except at Ra=10^6 for case 2 and 3, the isotherms on the left fills the cavity more than the one on the right. It may be noted that, the maximum temperature is 0.206, 0.163, 0.338 and 0.228 for cases 1, 2, 3 and 4, respectively at Ra = 10^5 whereas the corresponding values of maximum temperature are 0.132, 0.125, 0.196 and 0.217 at Ra = 10^6.

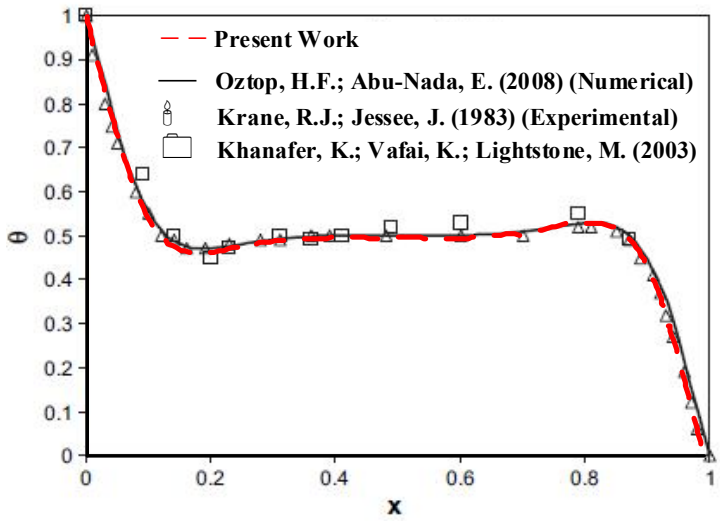

Fig. 2. Comparison between present work and other published data for the temperature distribution at the vertical mid section along the width of the enclosure (Ra = 10^5, Pr = 0.7).

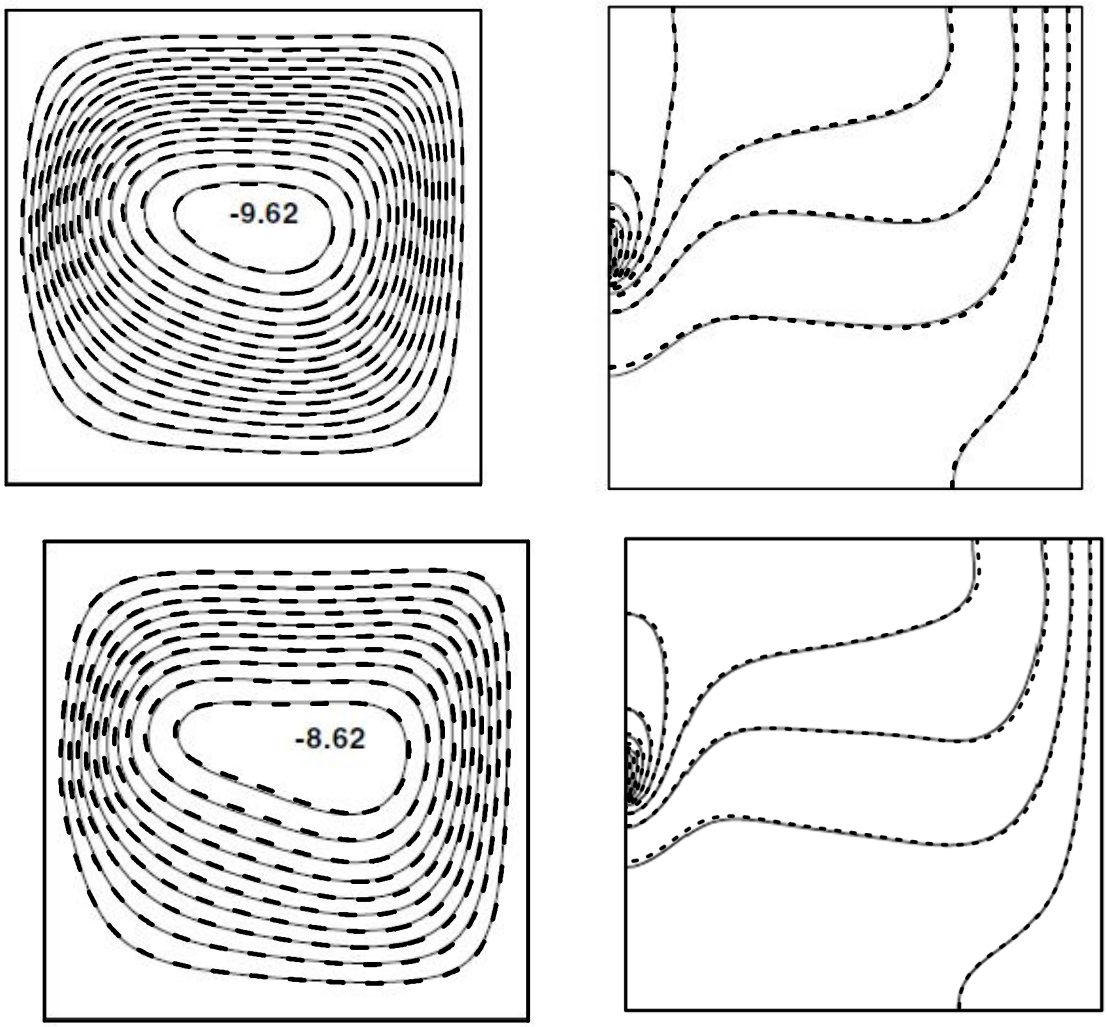

(a) $\phi = 0.2$

(b) $\phi = 0.1$

Fig. 3. Comparison of Streamlines (on the left) and isotherms (on the right) for Cu-water nanofluids with pervious numerical data Oztop, H.F.; Abu-Nada, E. (2008) at Ra = 10^5, $y_p = 0.5$, A = 1, h = 0.1, (a) $\phi = 0.2$, (b) $\phi = 0.1$.

Figs. 6 and 7 represents the streamlines and isotherms in the enclosure for the water based copper nanofluid case for various values of Rayleigh numbers and all cases at ϕ=0.1. As shown in Figs. 6 and 7, streamlines and isotherms for nanofluids and water show similar qualitative trends and the slight difference in magnitudes. As shown in Fig. 6, it must be noted that the contact line of the symmetrical circulation zones agrees with the axis of symmetry of the heat source for all Rayleigh numbers except at Ra=10^6 for case 3, the cell on the left fills the cavity more than the one on the right. It may be noted that, the maximum ψ= 3.43, 4.09, 5.31 and 0.374 for cases 1, 2, 3 and 4, respectively at Ra = 10^5 whereas the corresponding values of ψ are 13.33, 12.69, 23.42 and 1.95 at Ra = 10^6.

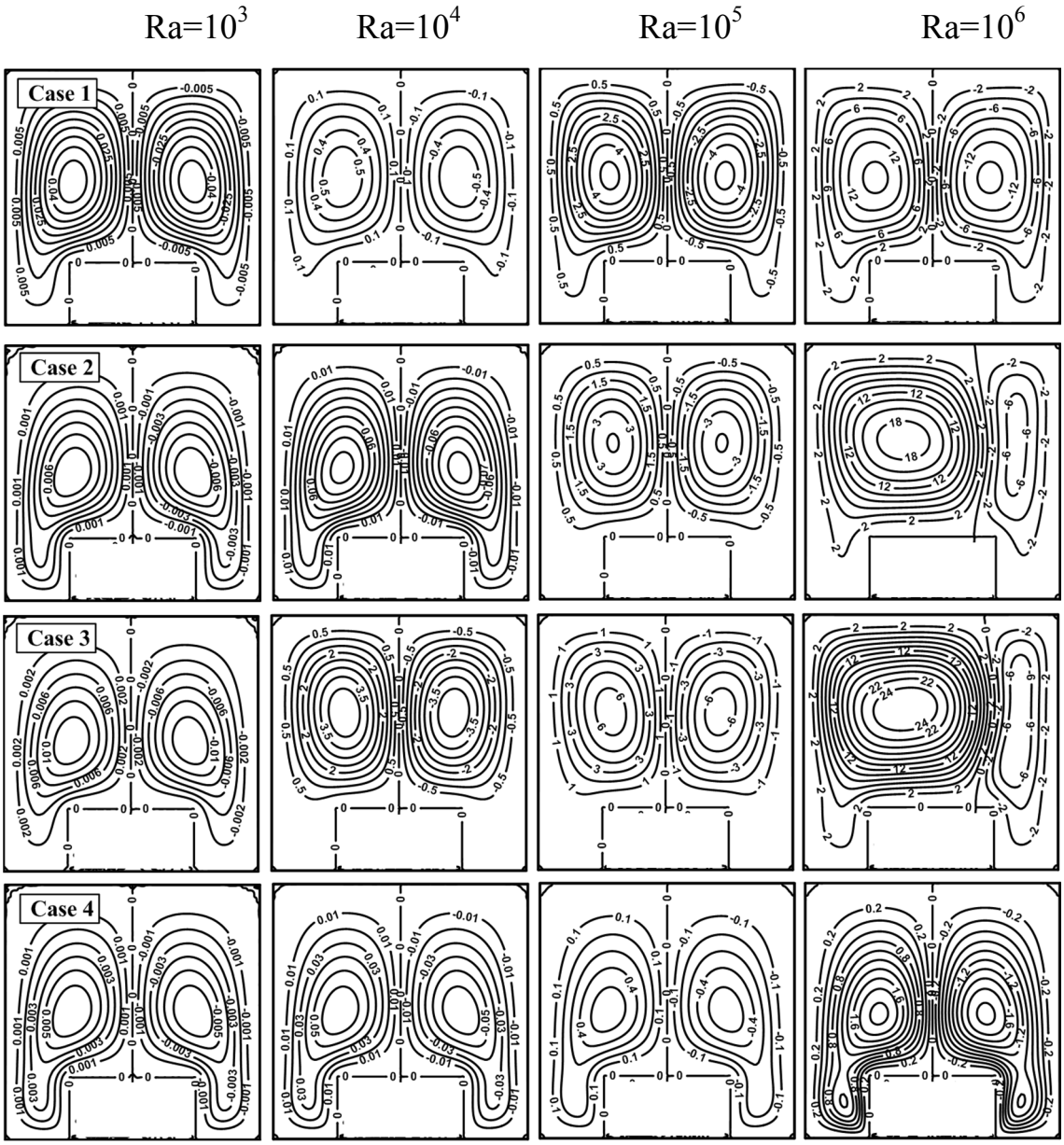

Fig. 4. Streamlines of the water fluid for various Rayleigh numbers and different cases at ϕ = 0.0.

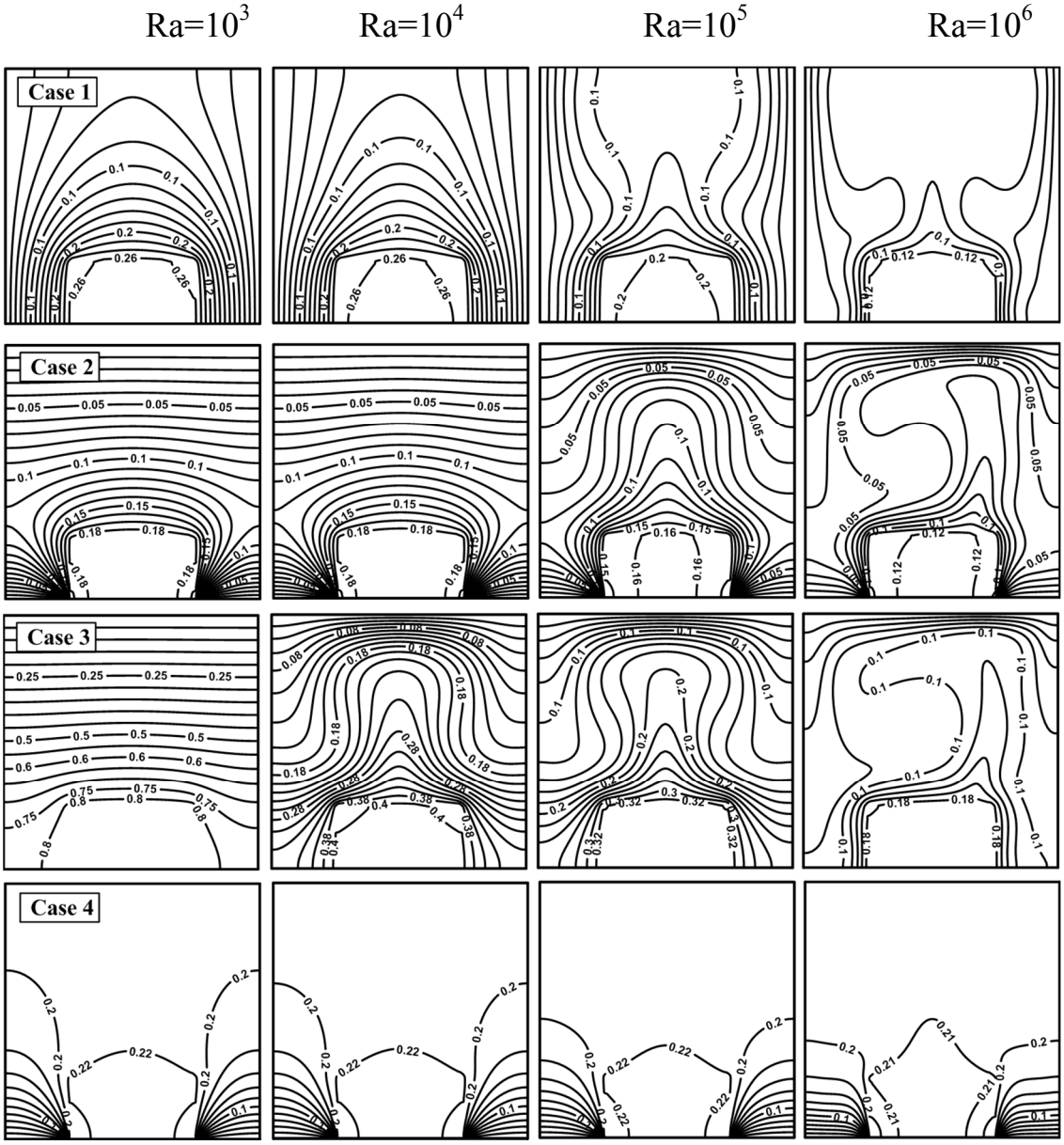

Fig. 5. Isotherms of the water fluid for various Rayleigh numbers and different cases at $\phi = 0.0$.

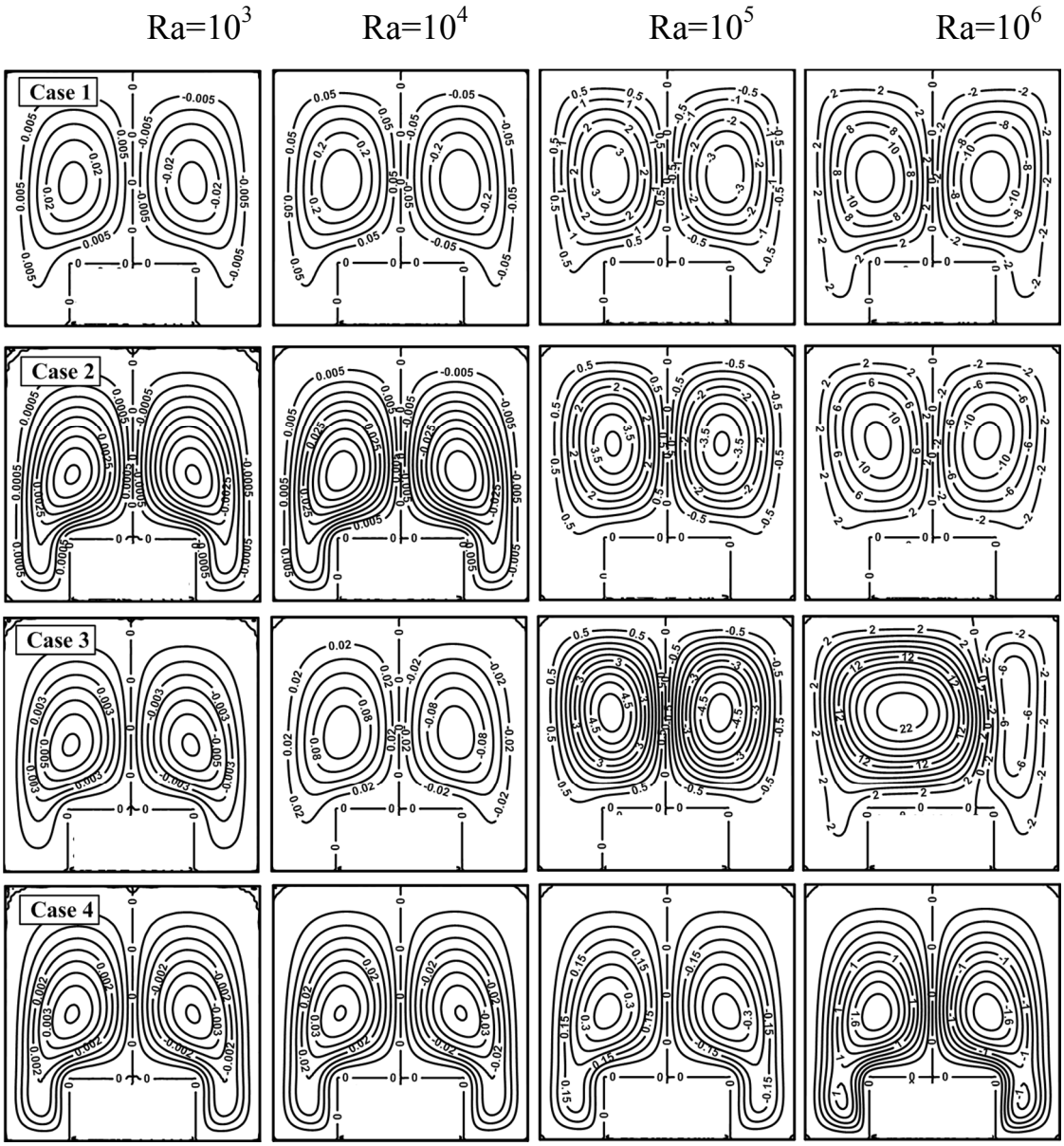

Fig. 6. Streamlines of a copper-based nanofluid for various Rayleigh numbers and different cases at $\phi = 0.1$.

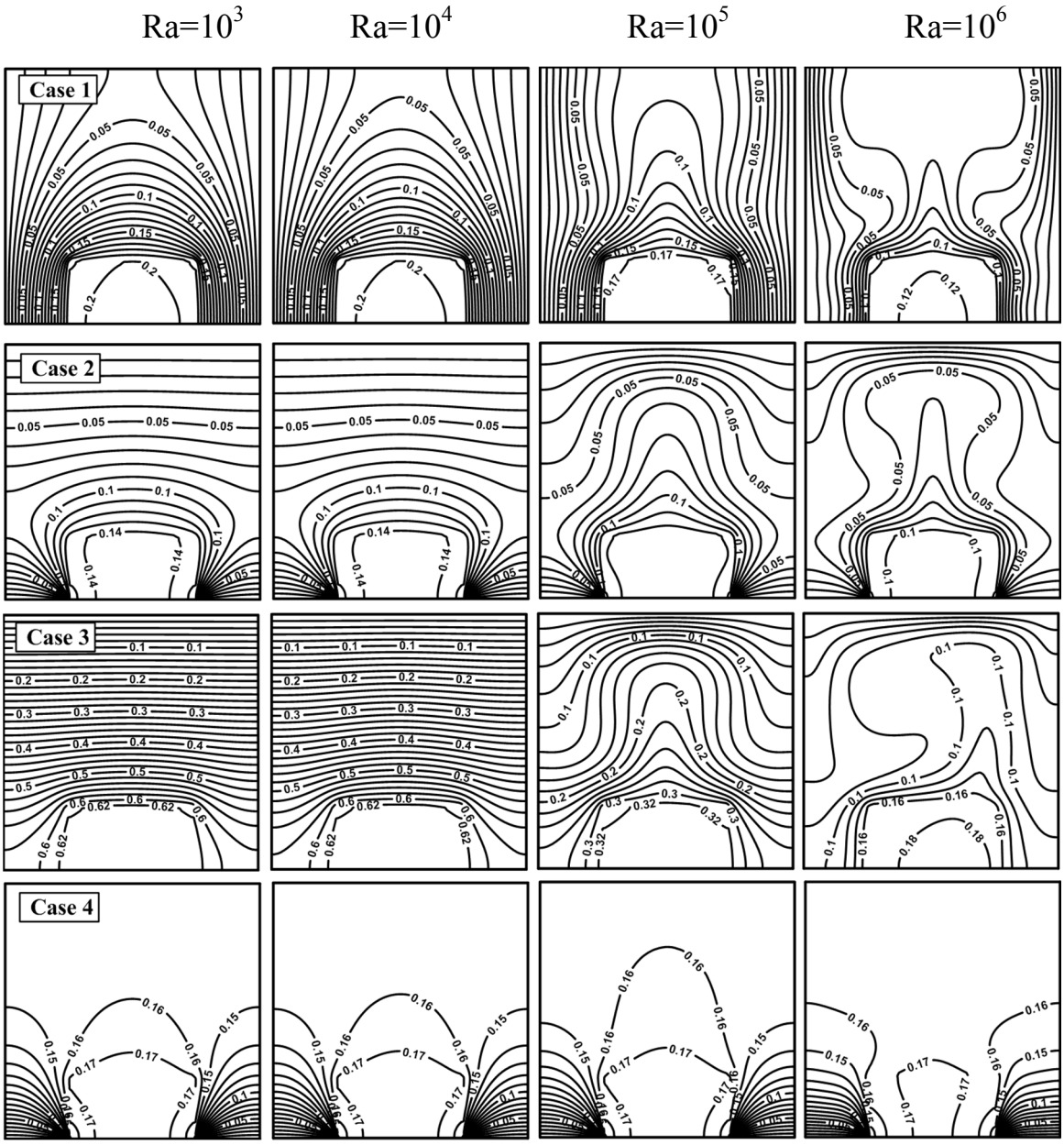

Fig. 7. Isotherms of a copper-based nanofluid for various Rayleigh numbers and different cases at ϕ = 0.1.

As shown in Fig. 7, the addition of nanoparticles to the base fluid enhances the thermal conduction and with increasing particle volume fraction for a given particle size, the enhancement increases. The enhancement of the thermal conduction should increase the convective heat transfer coefficient. It must be noted that the contact line of the symmetrical zones agrees with the axis of symmetry of the heat source for all Rayleigh numbers except at $Ra=10^6$ for case 2 and 3, the isotherms on the left fills the cavity more than the one on the right. It may be noted that, the maximum temperature is 0.18, 0.129, 0.331 and 0.179 for cases 1, 2, 3 and 4, respectively at $Ra = 10^5$ whereas the corresponding values of maximum temperature are 0.122, 0.106, 0.184 and 0.173 at $Ra = 10^6$.

Figs. 8 and 9 presented the streamlines and isotherms in the enclosure for the water based copper nanofluid case for various values of Rayleigh numbers and all cases at $\phi=0.2$. Figs. 8 and 9 show similar qualitative trends and the slight difference in magnitudes of streamlines and isotherms as increased of volume fraction. As shown in Fig. 8, it must be noted that the contact line of the symmetrical circulation zones agrees with the axis of symmetry of the heat source for all Rayleigh numbers except at $Ra=10^6$ for case 2 and 3, the cell on the left fills the cavity more than the one on the right. It may be noted that, the maximum ψ is 1.98, 0.386, 10.85 and 0.23 for cases 1, 2, 3 and 4, respectively at $Ra = 10^5$ whereas the corresponding values of ψ are 11.39, 9.81, 15.67 and 1.64 at $Ra = 10^6$.

As shown in Fig. 9, The addition of nanoparticles to the base fluid enhances the thermal conduction and with increasing particle volume fraction for a given particle size, the enhancement increases. The enhancement of the thermal conduction should increase the convective heat transfer coefficient. It must be noted that the contact line of the symmetrical zones agrees with the axis of symmetry of the heat source for

all Rayleigh numbers except at Ra=10^6 for case 2 and 3, the isotherms on the left fills the cavity more than the one on the right. It may be noted that, the maximum temperature is 0.153, 0.114, 0.21 and 0.141 for cases 1, 2, 3 and 4, respectively at Ra = 10^5 whereas the corresponding values of maximum temperature are 0.113, 0.092, 0.175 and 0.139 at Ra = 10^6.

As compare between Figs 4-9, it is clear that the flow and temperature patterns are influenced by the presence of nanoparticles. That is to say, the addition of nanoparticles to pure water reduces the strength of flow field. This reduction is more pronounced at low Rayleigh numbers where conduction heat transfer dominates. It is also apparent that as nanoparticles are added, the maximum dimensionless temperature is reduced which is an indication of enhancing the enclosure cooling performance. When volume fraction of nanoparticles increases from 0.0 to 0.2, length of the circulation cell becomes smaller and flow strength increases, as seen from Figs. 4, 6 and 8. It is also clear that an increase of Rayleigh number is associated with higher values of stream function and lower values of maximum temperature as a result of strengthening the buoyancy-induced flow field. Qualitatively similar trends in isotherms and streamlines are observed for nanofluids and water.

Fig. 10 shows the comparison of maximum temperature and average Nusselt number obtained from the heated block as function of Rayleigh number and volume fraction for all these cases. It can be clearly seen that the maximum temperature decreases with increasing Rayleigh number and volume fraction except case 4 is constant while the average Nusselt number increases with increasing Rayleigh number and volume fraction except case 4 is constant. Also, it is clear that the case 2 has the highest performance where the case 3 has the lowest one while case 1 and 4 are taking place between and this is valid for all values of Rayleigh number and volume

fraction. This tells that, for square enclosures, the enhancement in heat transfer, due to the presence of nanoparticles, is more pronounced at high Rayleigh number than at low Rayleigh number.

5.2. The effect of solid volume fraction:

Fig. 11 shows the variation of maximum temperature of the different value of Rayleigh number, and volume fraction. This figure shows a linear variation of the average Nusselt number with the volume fraction. As shown in this figure, as the Rayleigh number and volume fraction increases, the temperature gradients in boundary layer region near the walls increase. Also as noted from this figure, as Nanofluid volume fractions increase, the maximum temperature decrease too, since the thermal conductivity of the Nanofluid increases according to Eq. (11). The increase of solid volume fraction of nanoparticles causes the heat source maximum temperature to decrease particularly at low Rayleigh numbers where conduction is the main heat transfer mechanism. It is observed that the lowest maximum temperature is recorded when using case 2 for different value of Rayleigh number and volume fraction while, case 3 has the highest maximum temperature. The maximum temperature change relatively small at Ra = 10^3 and 10^4 while it changes at Ra = 10^5 and 10^6. The enhancement in the maximum temperature when the volume fraction of nanoparticles is increased from 0 to 0.2, at Ra = 10^3, is approximately 39.4% whereas the enhancement is around 26.2% at Ra = 10^6 for case 2.

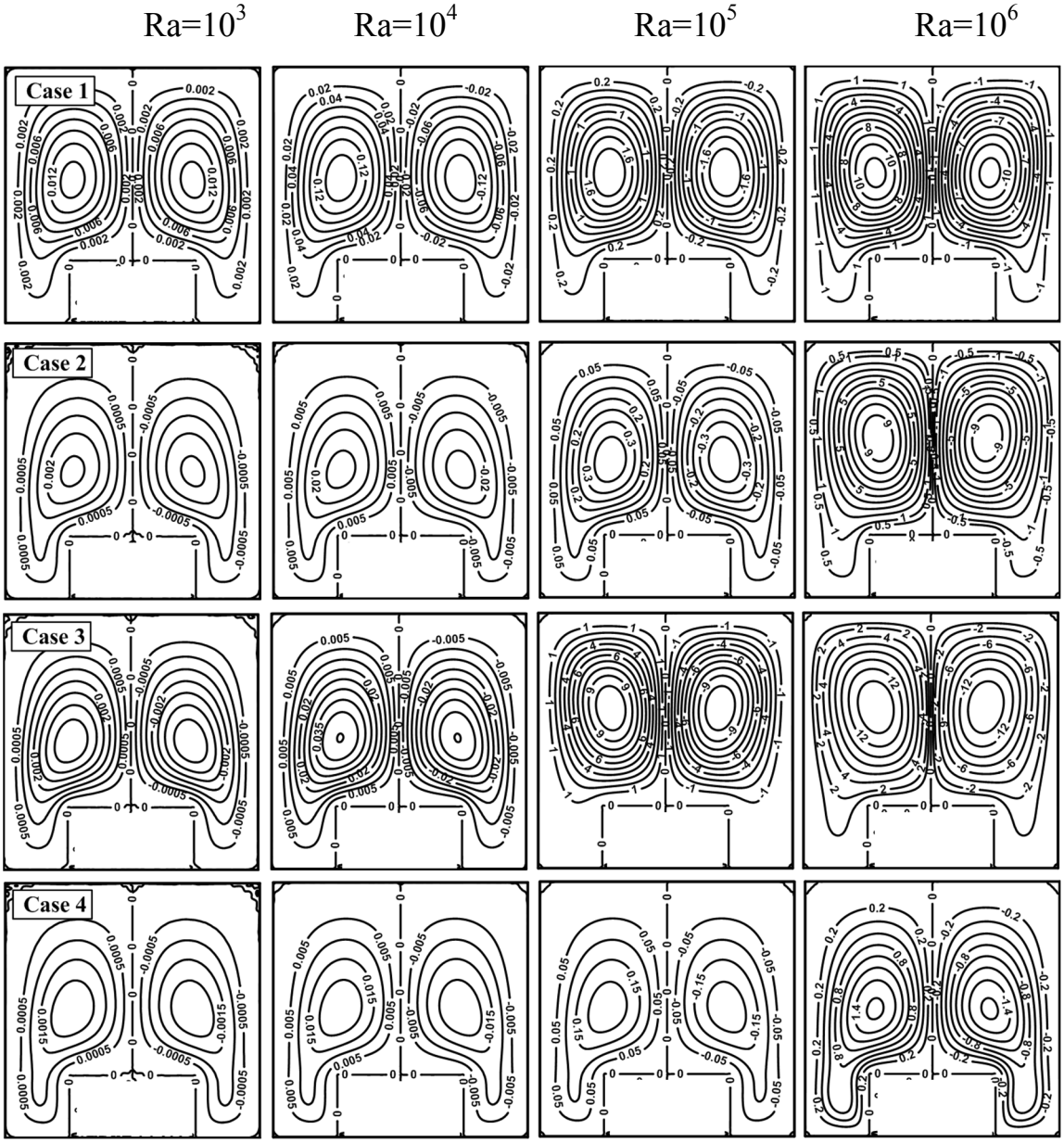

Fig. 8. Streamlines of a copper-based nanofluid for various Rayleigh numbers and different cases at $\phi = 0.2$.

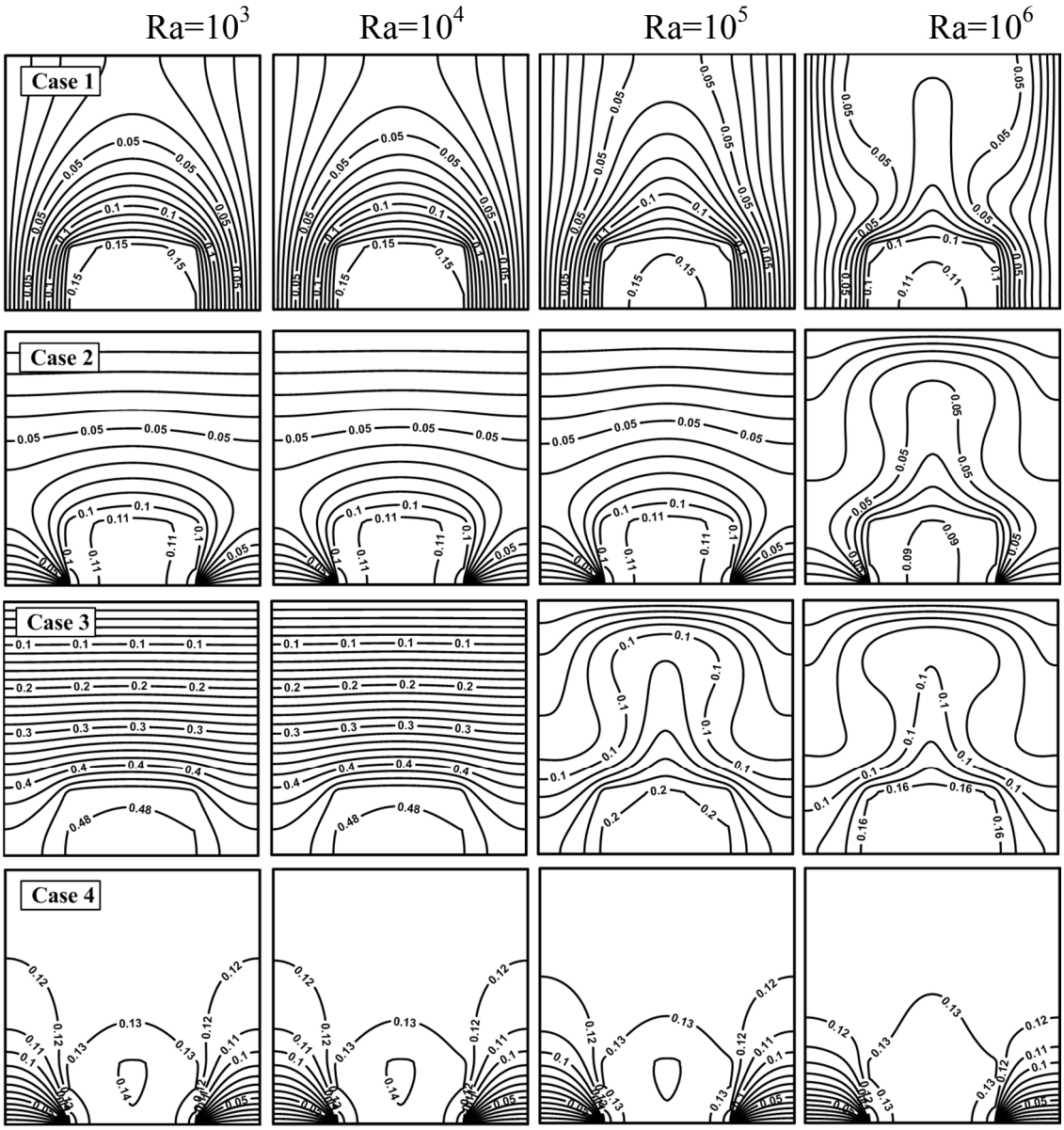

Fig. 9. Isotherms of a copper-based nanofluid for various Rayleigh numbers and different cases at ϕ = 0.2.

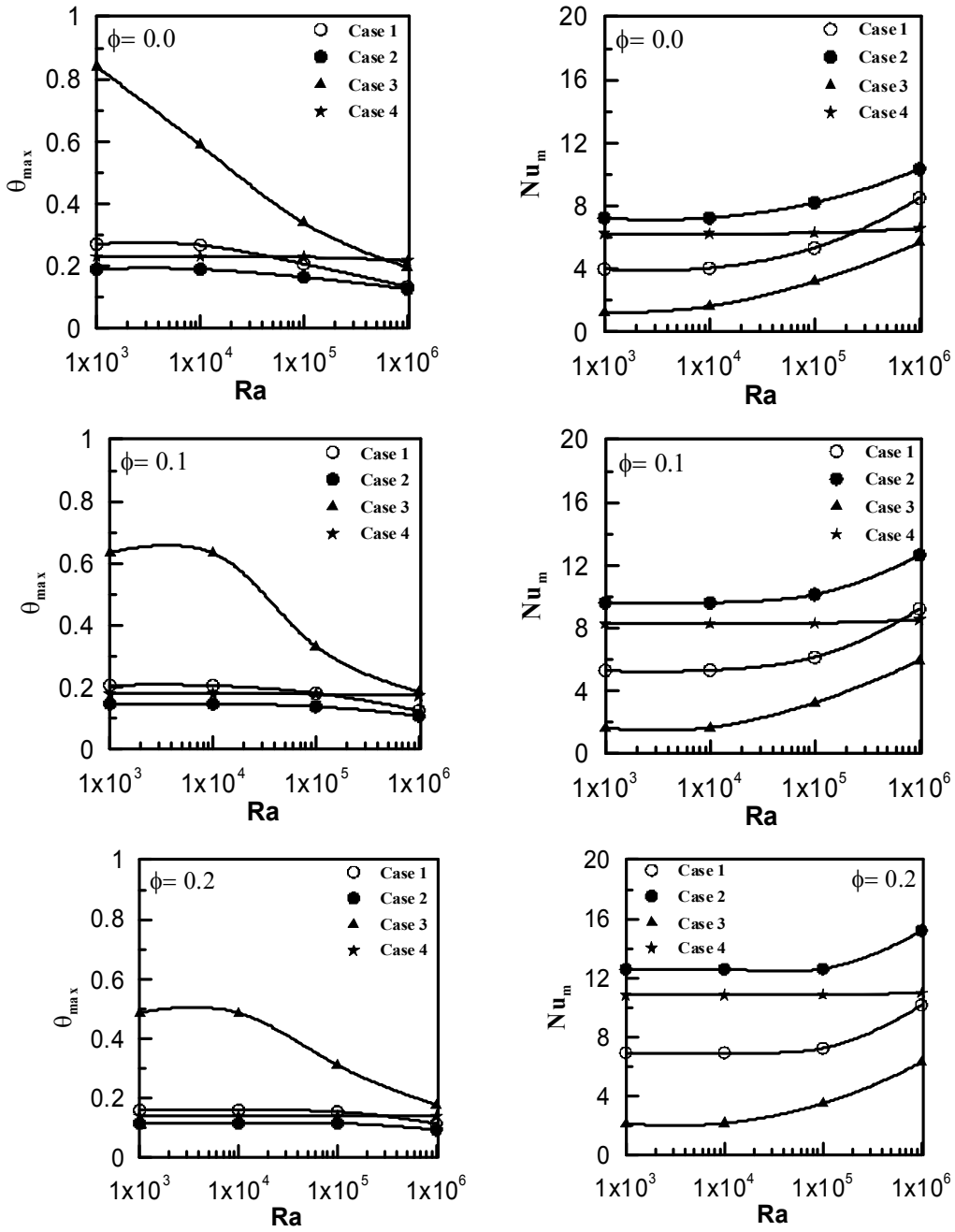

Fig. 10. Variation of maximum temperature and average Nusselt number for Rayleigh number for different volume fractions, Cu-water nanofluid.

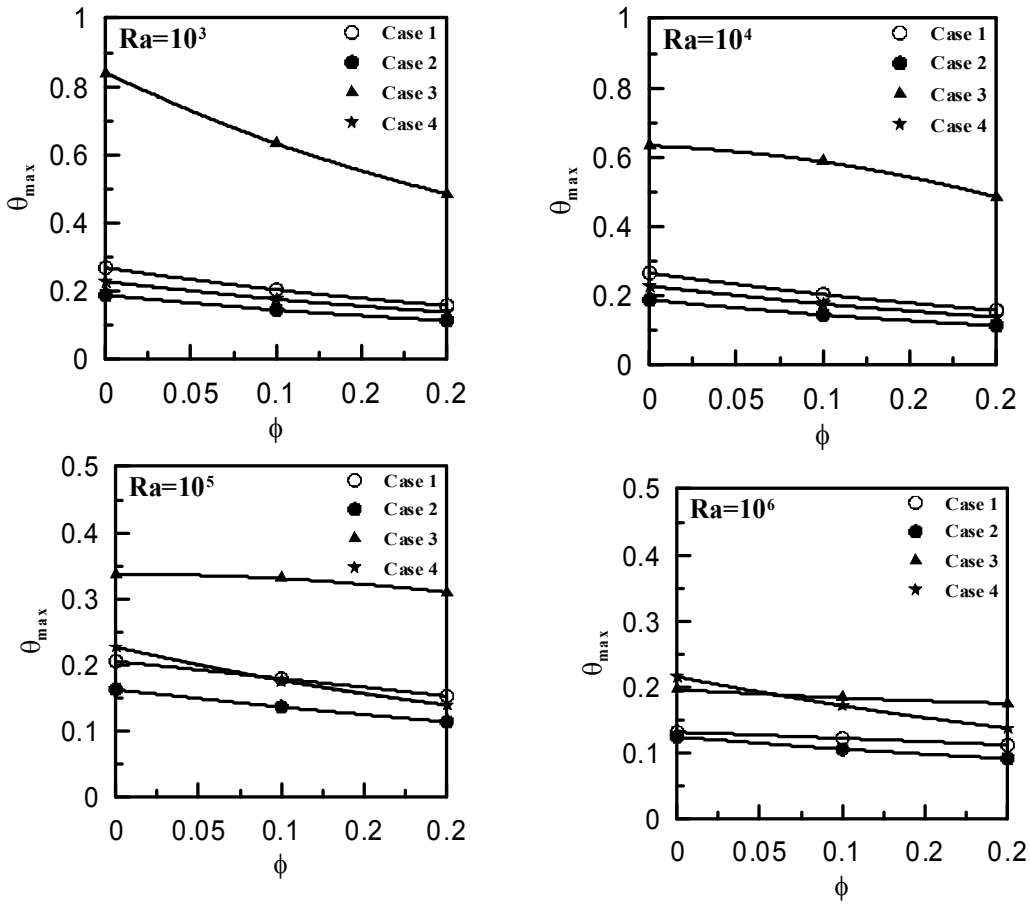

Fig. 11 Variation of the maximum temperature for different Rayleigh numbers and volume fraction.

5.3. The effect of the type of nanofluid:

Fig. 12 compares the isotherms using different nanofluids as Cu-water, Al_2O_3-water and TiO_2-water for different Rayleigh numbers at ϕ = 0.1 and 0.2. For both nanofluids, isotherms show almost the same distribution for these three nanofluids due to closer value of thermal conductivity of Cu, Al_2O_3 and TiO2 which is given in Table 1. Overall observation of Fig. 12 shows that as the volume fraction and Rayleigh number increase, the isotherms decrease due to the movements of particles

become irregular and random, because of the increase of energy exchange rates in the fluid.

Fig. 13 illustrates the effects of Rayleigh numbers, type of nanoparticle and volume fraction on maximum temperature and average Nusselt number for case 2. The figure shows that when Rayleigh number increases, the maximum temperature decreases and average Nusselt number increases for all volume fraction and nanofluids because heat transfer coefficient is proportional to the thermal conductivity of all types of nanofluids, which is increasing with volume fraction. This is an indication that the presence of nanoparticles clearly enhance heat absorption of the heated block causing its temperature to decrease. In general, these enhancements are due to higher thermal conductivity of nanoparticles and the role of Brownian motion of nanoparticles on enhancement of thermal conductivity which is due to larger surface area of nanoparticles for molecular collisions. The difference for maximum temperature and mean Nusselt number becomes larger especially at higher Rayleigh numbers as volume fraction of nanoparticles increases due to increase heat transfer by dominate of convection mode. At ϕ= 0.2, the maximum temperature and average Nusselt number is constant for $Ra \leq 10^5$ after this value the maximum temperature decreases and average Nusselt number increases. Also as noted this figure, the lowest heat transfer is obtained for TiO_2 due to domination of conduction mode of heat transfer since TiO_2 has the lowest value of thermal conductivity compared to Cu and Al_2O_3. However, the difference in the values of Al_2O_3 and Cu is negligible. The highest heat transfer is recorded when using Cu-nanofluids for all Rayleigh number and volume fraction.

6. Conclusions:

Natural convection heat transfer around heated block in enclosure filled with different types of nanofluids has been numerically investigated. The effects on the enclosure cooling performance of Rayleigh number, the volume fraction and the type of nanoparticle, and the local cooling walls of the enclosure are studied for four cases. The important concluding remarks are presented below:

- As Ra increases, the buoyant force becomes stronger and velocity increases, also the isotherms are deformed due to convection mode being to play a more significant role with increasing the flow velocity.
- The flow and temperature patterns are influenced by the presence of nanoparticles.
- Qualitatively similar trends in isotherms and streamlines are observed for nanofluids and water.
- The enhancement in heat transfer, due to the presence of nanoparticles, is more pronounced at high Rayleigh number than at low Rayleigh number.
- Case 2 has the highest cooling performance for different values of Rayleigh number and volume fraction while, case 3 has the lowest cooling performance for Cu nanoparticle.
- The enhancement in the maximum temperature for case 2 when the volume fraction of nanoparticles is increased from 0 to 0.2, at Ra = 10^3, is approximately 39.4% whereas the enhancement is around 26.2% at Ra = 10^6 for Cu nanoparticle.
- The highest heat transfer is recorded when using Cu-nanofluids for all Rayleigh numbers and volume fractions.

- At ϕ= 0.2 and case 2, the maximum temperature and average Nusselt number is constant for Ra $\leq 10^5$ after this value the maximum temperature decreases and average Nusselt number increases for the considered nanoparticles.

References:

1- *Abu-Nada, E. (2010): Effects of variable viscosity and thermal conductivity of CuO-Water nanofluid on heat transfer enhancement in natural convection: mathematical model and simulation, J. Heat Transfer, vol. 132, 052401 (9 pages).*

2- *Abu-Nada, E.; Masoud, Z.; Hijazi, A. (2008): Natural convection heat transfer enhancement in horizontal concentric annuli using nanofluids. Int. Commun. Heat Mass Transfer, vol. 35, pp. 657–665.*

3- *Abu-Nada, E.; Masoud, Z.; Oztop, H.F.; Campo, A. (2010): Effect of nanofluid variable properties on natural convection in enclosures. International Journal of Thermal Sciences, vol. 49 479–491*

4- *Aminossadati, S.M.; Ghasemi, B. (2011): Enhanced natural convection in an isosceles triangular enclosure filled with a nanofluid. Computers Mathematics Appli- cations, vol. 61, pp. 1739–53.*

5- *Aminossadati, S.M.; Ghasemi, B. (2009): Natural convection cooling of a localized heat source at the bottom of a nanofluid-filled enclosure, Eur. J. Mech. B/Fluids, vol. 28, pp. 630-640.*

6- *Aminossadati, S.M.; Ghasemi, B. (2011): Natural convection of water–CuO nanofluid in a cavity with two pairs of heat source–sink. International Communications in Heat and Mass Transfer, vol. 38, pp. 672–8.*

7- *Daungthongsuk, W.; Wongwises, S. (2007): A critical review of convective heat transfer of nanofluids, Renew. Sustain. Energy Rev., vol. 11, pp. 797-817.*
8- *El-Agouz, S.A. (2008): The effect of internal heat source and opening locations on environmental natural ventilation. Energy and Buildings, vol. 40, pp. 409–418.*
9- *Ghasemi, B.; Aminossadati, SM. (2010): Brownian motion of nanoparticles in a triangular enclosure with natural convection. International Journal of Thermal Science, vol. 49, pp. 931–40.*
10- *Ghasemi, B.; Aminossadati, SM. (2010): Periodic natural convection in a nanofluid- filled enclosure with oscillating heat flux. International Journal of Thermal Science, vol.49, pp. 1–9.*
11- *Hwang, K.S.; Lee, J.H.; Jang, S.P. (2007): Buoyancy-driven heat transfer of water based Al2O3 nano-fluids in a rectangular cavity, International Journal of Heat and Mass Transfer, vol. 50, pp. 4003-4010.*
12- *Jou, R.; Tzeng, S. (2006): Numerical research of nature convective heat transfer enhancement filled with nano-fluids in rectangular enclosures, International Communications in Heat and Mass Transfer, vol. 33, pp. 727-736.*
13- *Khanafer, K.; Vafai, K.; Lightstone, M. (2003): Buoyancy driven heat transfer enhancement in a two-dimensional enclosure utilizing nano-fluids, International Journal of Heat and Mass Transfer, vol. 46, pp. 3639-3653.*
14- *Kleinstreuer, C.; Feng, Y. (2011): Experimental and theoretical studies of nanofluid thermal conductivity enhancement: a review, Nanoscale Res. Lett., vol. 6, pp. 1-13.*

15- *Krane, R.J.; Jessee, J. (1983): Some detailed field measurements for a natural convection flow in a vertical square enclosure, in: 1st ASME-JSME Thermal Engineering Joint Conference, vol. 1, pp. 323–329.*
16- *Ögüt, EB. (2009): Natural convection of water-based nanofluids in an inclined enclosure with a heat source. International Journal of Thermal Sciences, vol.48, pp. 2063–73.*
17- *Oztop, H.F.; Abu-Nada, E. (2008): Numerical study of natural convection in partially heated rectangular enclosure filled with nanofluids. Int. J. Heat Fluid Flow, vol. 29, pp. 1326–1336.*
18- *Patankar, S.V. (1980): Numerical Heat Transfer and Fluid Flow, Hemisphere Publishing Company, New York,.*
19- *Sheikhzadeh, GA. ; Arefmanesh, A.; Kheirkhah, MH.; Abdollahi, R. (2011): Natural convection of Cu–water nanofluid in a cavity with partially active side walls. European Journal of Mechanics B/Fluids, vol. 30, pp. 166–76.*
20- *Trisaksri, V.; Wongwises, S. (2007): Critical review of heat transfer characteristics of nanofluids, Renew. Sustain. Energy Rev., vol. 11, pp. 512-523.*
21- *Versteeg, H.K.; Malalasekera, W. (2007): An Introduction to Computational Fluid Dynamics the Finite Volume Method, JohnWiley & Sons Inc., New York, Second edition published.*

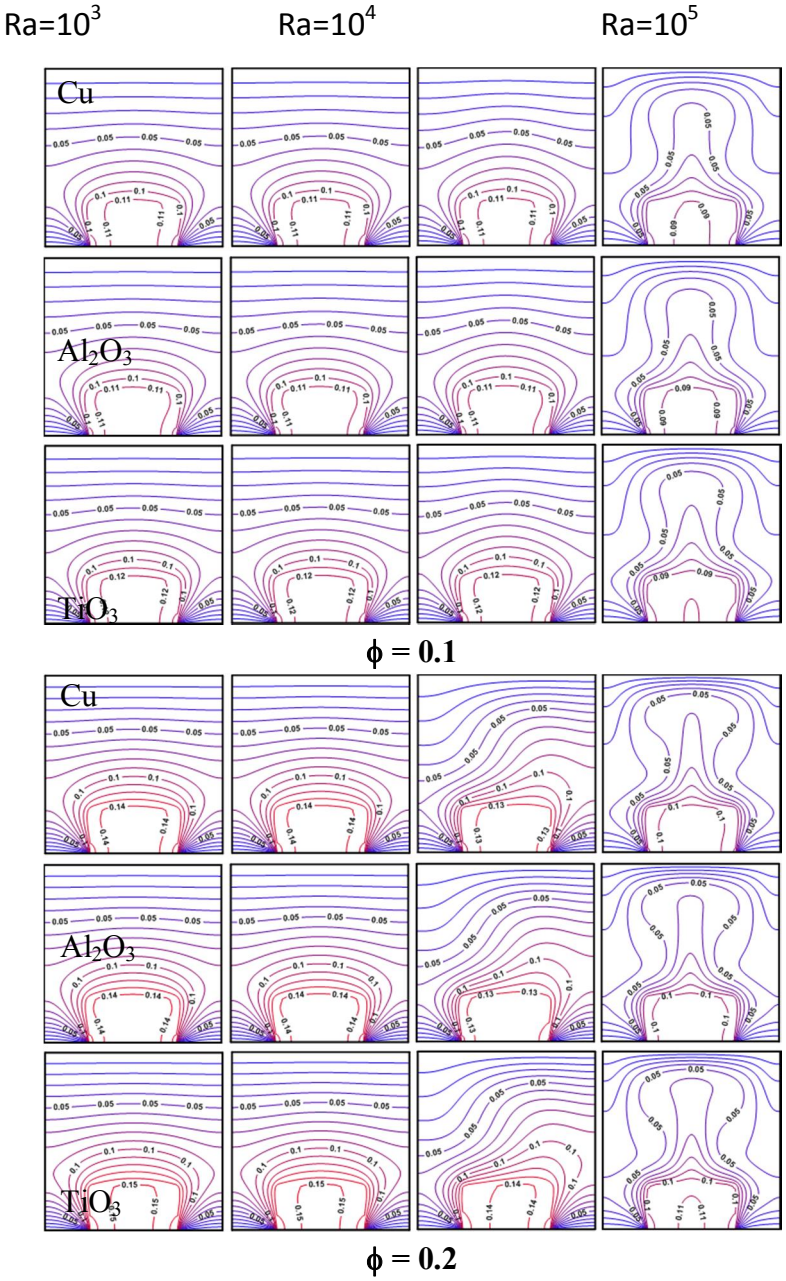

Fig. 12. Isotherms of different nanoparticles for various for different Rayleigh numbers at ϕ = 0.1 and 0.2 for case 2.

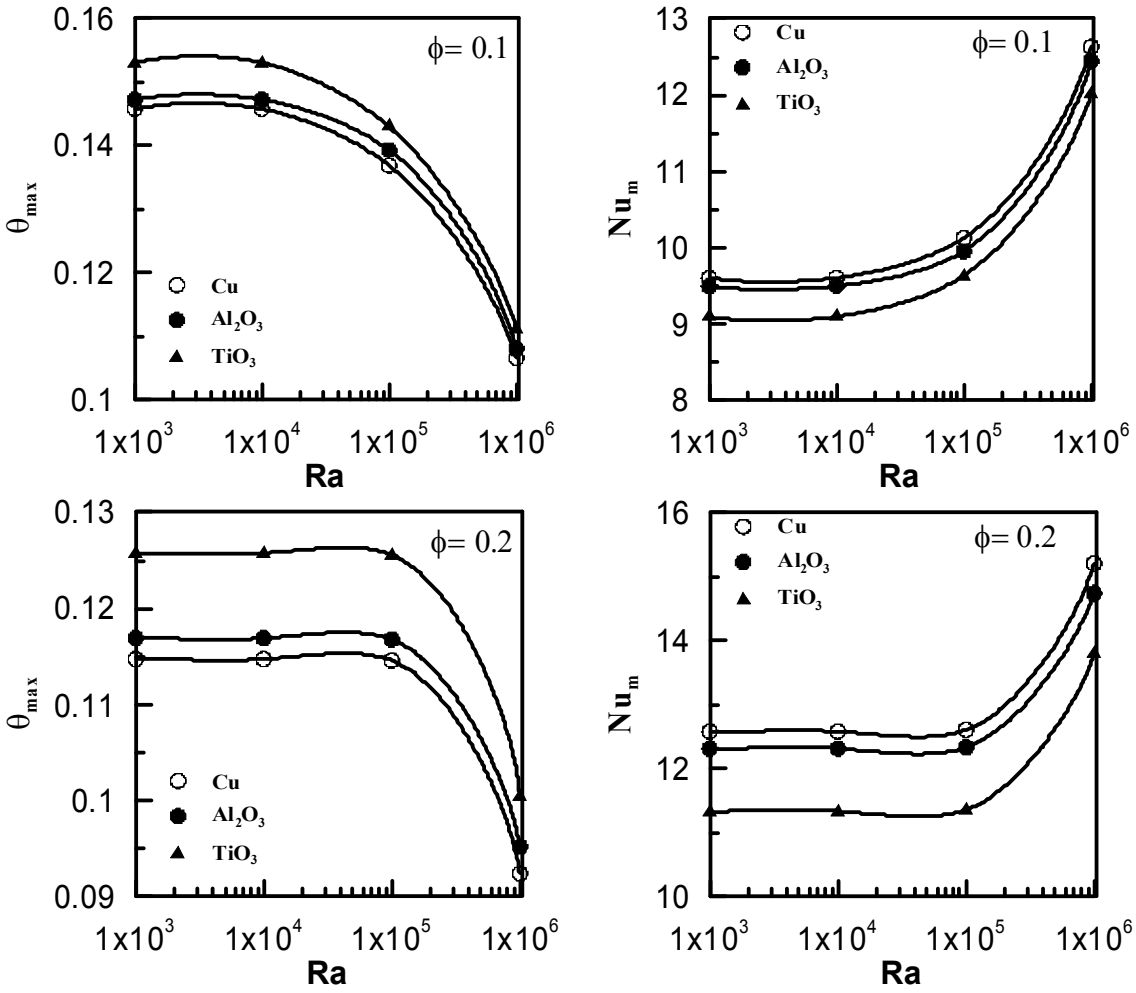

Fig. 13 Variation of the maximum temperature and average Nusselt number of different nanoparticles for different Rayleigh numbers and volume fraction for case 2.